Magnetic properties of Ising thin films with cubic lattices

Y. Laosiritaworn,[1] J. Poulter,[2] and J. B. Staunton[3]
[1]*Department of Physics, Faculty of Science, Chiang Mai University, Chiang Mai 50200, Thailand*
[2]*Department of Mathematics, Faculty of Science, Mahidol University, Bangkok 10400, Thailand*
[3]*Department of Physics, University of Warwick, Coventry CV4 7AL United Kingdom*
(Received 11 July 2003; revised manuscript received 4 December 2003; published 22 September 2004)

We have used Monte Carlo simulations and mean-field analysis to observe the magnetic behavior of Ising thin films with cubic lattice structures as a function of temperature and thickness, especially in the critical region. Magnetization and magnetic susceptibility, including layer variation, are investigated. We find that the magnetic behavior changes from two-dimensional to three-dimensional character with increasing film thickness. Both the crossover of the critical temperature from a two-dimensional to a bulk value and the shift exponent are observed. Nevertheless, with support from a scaling function, the simulations show that the effective critical exponents for films with large enough layer extents only vary a little from their two-dimensional values. This, in particular, provides an indication of two-dimensional universality in the thin films.

DOI: 10.1103/PhysRevB.70.104413 PACS number(s): 75.40.Cx, 64.60.Fr, 75.40.Mg, 75.70.Ak

I. INTRODUCTION

The dimensional crossover of magnetic properties from two-dimensional (2D) to three-dimensional (3D) character in magnetic multilayers has currently attracted much interest as a result of both technological and fundamental importance.[1,2] Of particular interest is the critical behavior of magnetic thin films for which the dimensionality d is not well established. It is interesting to consider how magnetic properties such as the magnetization m, magnetic susceptibility χ, and critical temperature T_C depend on the thickness of the film.

Critical temperatures T_C in multilayered systems are known to change from 2D to 3D values with increasing numbers of layers. Magnetic films, however, should belong to a 2D universality class owing to the correlation lengths (ξ) being constrained by the film thickness and allowed to expand only in the in-plane direction. This is not apparent from well-known experimental studies of thin films of nickel[6] which provide evidence of a dimensional crossover of the critical exponent β from 2D to 3D. Here, we try to clarify this discrepancy by carrying extensive Monte Carlo simulations of simple cubic (sc), body-centered-cubic (bcc), and face-centered-cubic (fcc) coordinated thin films.

Both theoretical[3,4] and experimental[5–7] investigations show that the Ising model is very useful for the study of critical behavior in thin ferromagnetic films. Various techniques have been used.[8–17] Magnetic profiles, T_C, the shift exponent,[8–12] and the effective exponent dependence on thickness and temperature away from T_C (Ref. 13) have been studied together with the dimension change using scaling functions of thick films around the bulk T_C (Ref. 14), and how the effective critical exponents in thin films depend on thickness at the film critical point.[15–17] There are nonetheless some important issues which remain unresolved; for example, the confirmation of universality in different structures with the same thickness, the confirmation of the effective exponents via scaling functions, the empirical form for the observation of the convergence of the shift exponent to the bulk limit from both Monte Carlo and mean-field studies, the possibilities in using Ising thin films to describe real experiments, etc.

Consequently, in this study, we aim to give a more complete picture of the magnetic phase transition in thin films in all cubic structures especially at the critical point. We first investigate how the magnetic properties, including their layer resolution, depend on temperature and thickness by means of Monte Carlo simulations and mean-field theory. Second, we calculate T_C, following it to the bulk limit. Then, using an empirical fit, we extract the shift exponents and their convergence to the 3D value. Next, with (empirical) finite-size scaling forms, we extract the effective critical exponents as a function of thickness l. After that, we construct various kinds of data collapsing to confirm the results and to observe how the exponents depend on the forms of the scaling functions. Finally, we discuss our results and compare the characteristic effective critical exponents with those found in experiments.

II. METHODOLOGY

In this study, we consider the Ising hamiltonian $H=-J\Sigma_{\langle ij\rangle} S_iS_j$, where the spin S_i takes on the values ±1 and the sum includes only first nearest-neighbor (1 NN) pairs. Helical (periodic) and free boundary conditions are used for the in-plane and out-of-plane directions, respectively. We use units of J/k_B and J for temperatures and energies, respectively, with the magnetization per spin defined as $m=(1/N)\Sigma S_i$ where N is total number of spins.

The simulations are carried out for sc, fcc, and bcc films of size $N=L\times L\times l$ where $L\times L$ represents the number of sites (spins) in each layer of the film and l is the number of layers. We vary L from 64 to 128 (in steps of 8) with l ranging from a monolayer (bilayer for bcc films) to 20 layers. The spin configurations of the films are updated using the Wolff algorithm[18] to minimize statistical errors arising from correlation time.[19,20] The random number generator (drand48) is chosen carefully.[21–23] During a simulation, the magnetization per spin, m, and the energy E are measured when the number of flipped spins exceed or is equal to N.

Each simulation is found to reach its equilibrium before 30 MCS (Monte Carlo step per site). To ensure equilibration, we wait at least 3000 MCS (about 100 times the equilibration time) from its initial state (disordered state) before taking any measurements. The expectation value of the square of the statistical error of an observable, e.g., m, takes the form[19]

$$\langle(\delta m)^2\rangle = \frac{1}{n}(\langle m^2\rangle - \langle m\rangle^2)\left(1 + 2\frac{\tau}{\delta t}\right), \tag{1}$$

where, at large enough n, $\tau = \Sigma_{i=1}^{n}(\langle m_0 m_i\rangle - \langle m\rangle^2)/(\langle m\rangle^2 - \langle m\rangle^2)$ is the integrated correlation time,[19] δt is the time interval between two successive configurations—i.e., about 1 MCS—and n is the number of configurations being sampled. Since $(\langle m_0 m\rangle - \langle m\rangle^2)/(\langle m^2\rangle - \langle m\rangle^2)$ decays with time, by resampling the spin configurations with the time interval between two successive data being much greater than τ or at least 2τ,[27] it can be assumed that the correlation between two successive configurations sampled in this new interval is minimized or can be discarded. Our results show τ to increase with both size $L \times L$ and thickness l of the film. In our biggest system $128 \times 128 \times 20$, $\tau < 4$ MCS.

Once τ has been calculated for each system, at least $n' = 5 \times 10^5$ configurations sampled in the interval 2τ are used to calculate the expectation of the magnetization per spin, $\langle m\rangle = (1/n')\Sigma_i^{n'}|m_i|$, as well as the magnetic susceptibility $\chi = \beta N(\langle m^2\rangle - \langle|m|\rangle^2)$ where $\beta = J/k_B T$. Similarly, the layer dependence of these magnetic properties, m_k and χ_k, where k is a layer index, are calculated to observe the surface effects upon the magnetic properties. The critical temperature T_C is located via the fourth-order cumulant U_L (Ref. 24):

$$U_L = 1 - \frac{1}{3}\frac{\langle m^4\rangle}{\langle m^2\rangle^2}, \tag{2}$$

where, at $T = T_C$, U_L should be independent of L; i.e., for differing sizes L and L', $(U_L/U_{L'})_{T=T_C} = 1$. Owing to finite-size effects, $T_C(b = L/L')$ is plotted against $(\ln b)^{-1}$, and the results in the infinite limit are obtained at $(\ln b)^{-1} \to 0$.[24] To maximize the efficiency of this T_C calculation, for each thickness, we perform a single long simulation at a temperature T_0 and use the histogram method[25,26] to extrapolate U_L to a temperature nearby in order to find the cumulant crossing point on a fine scale. The temperature T_0 is chosen to be that at the peak of the susceptibility curve for the $L = 128$ system, and approximately $1-4 \times 10^6$ spin configurations are used to create the histograms. To exclude the data obtained from temperatures too far from the simulated temperature T_0, the range of extrapolation $|T - T_0|$ is restricted by the criterion $|U(T) - U(T_0)| \leq \sigma_E$,[27] where $U = \langle E\rangle$, the average of the energy, and σ_E is a standard deviation of E at T_0.

We consider an empirical finite size scaling form for film geometry[16,17] to find how m and χ scale with the size L and thickness l of the systems and use this to extract the effective critical exponents from our results. The basic finite-size scaling ansatz[28–33] rests on an assumption that only a single correlation length ξ is needed to describe the critical properties of thin films. Hence the empirical scaling forms for m and χ at some fixed l's can be written as[16,17]

$$\langle m(T,l)\rangle = L^{-\beta'/\nu'}\tilde{m}(L^{1/\nu'}t, l),$$

$$\chi(T,l) = L^{\gamma'/\nu'}\tilde{\chi}(L^{1/\nu'}t, l), \tag{3}$$

where γ', β', and ν' are the effective critical exponents associated with χ, m, and ξ, respectively. For $l = 1$ or the monolayer system, the effective exponents are the critical exponents for the 2D system. The functions $\tilde{\chi}$ and $\tilde{m}$ are scaling functions for a given l and $t = T/T_C(l) - 1$ is the reduced temperature. These scaling functions for a range of L should collapse onto a single curve with the correct critical temperature and effective critical exponents. The effective exponent $1/\nu'$ can be extracted from the derivative of the cumulant with respect to L at T_C owing to its variation with system size as $L^{1/\nu'}$.[24] Note that if Eq. (3) correctly encapsulates the nature of magnetic critical behavior in films, we can extract the effective exponents β'/ν' and γ'/ν' from the slopes of the log-log plots of m or χ against L at T_C. To continue with confidence, we believe it is necessary to demonstrate the validity of the finite-size scaling, Eq. (3), in modeling results from our calculations. This can be done by establishing the following:

(i) According to Eq. (3), at T_C, a log-log plot of χ or m against L should be linear.

(ii) Based on the hyperscaling relation $\gamma/\nu + 2\beta/\nu = d$,[34] it is possible to consider the effective dimensionality $d_{\text{eff}} = \gamma'/\nu' + 2\beta'/\nu'$.[16,35] For $l/L \ll 1$, we expect 2D-like behavior; i.e., d_{eff} should stay close to 2.[16]

(iii) With suitable effective exponents in the critical region, a scaling function for any L but a particular l—i.e., Eq. (3), should collapse onto a single curve. This will confirm the reliability of the effective exponents extracted from our simulations

III. RESULTS AND DISCUSSION

A. Magnetization and magnetic susceptibility

From magnetization m and susceptibility χ profiles for various film thicknesses l and system sizes L the crossover of behavior from 2D like for the monolayer (bilayer in bcc) to 3D like for films with 20 or more layers is found. The transition point moves from 2D to 3D values with increasing film thickness in a good agreement with previous studies.[12,13] Furthermore, the layer resolution shows the m and χ magnitudes to increase from the lowest values for the surface layer the largest values in the interior of the films.

Such layer variation is expected because the exchange ferromagnetic energy associated with each spin is greater in the bulk than at the surfaces owing to the increase in numbers of nearest neighbors. This effect shows up in the simulations. The probability for a site getting updated is $D(i,j,k) = (1/M)\Sigma_{n=1}^{M} s'(i,j,k)$, where $s'(i,j,k)$ is the number of times the site at location (i,j,k) is in a Wolff update, and M is the total number of clusters forming (flipping) in a simulation. We find that, at any finite temperature in the fer-

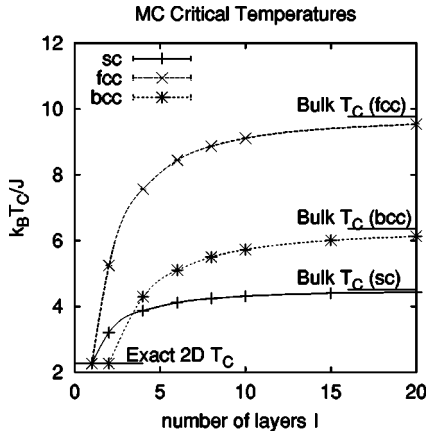

FIG. 1. The critical temperatures T_C as a function of thickness l extracted from Monte Carlo simulations.

romagnetic phase, D at the surface layers always has the lowest magnitude, showing that spins which belong to the majority direction are preferentially located in the inner layers rather than near the surface. Hence, at the surface layers, there will be some (minority direction) spins behaving as a buffer which results in smaller m magnitude. Similarly, for χ, the "buffer" in the surface layers helps to reduce the magnetic fluctuations leading to a smaller χ than those in the inner layers.

The same qualitative trends are also uncovered by using a mean-field approximation.[36] Again the evolution of the magnetic properties from 2D to 3D like is found and the smallest m and χ values lie on the surface and highest for the innermost layers.

B. Critical temperatures and shift exponents

We calculate the critical temperatures of the films from our Monte Carlo simulations using the cumulant method.[24] We find a change from 2D to bulk values as l is increased. Figure 1 shows evidence of such a dimensional crossover for the Ising thin films. Both our 2D and bulk results agree very well with the exact Ising 2D results and previous Ising 3D studies.[26,37] As the number of layers is increased, the critical temperature moves towards the 3D value owing to the increase of the average exchange interaction energy. On similar grounds, for $l \geqslant 4$, we find $T_C^{\mathrm{sc}}(l) < T_C^{\mathrm{bcc}}(l) < T_C^{\mathrm{fcc}}(l)$. Mean-field estimates are consistently higher than those from these Monte Carlo results and agree well with a previous calculation.[38]

We also investigate the shift exponents λ. Generally λ can be written in terms of a power law

$$1 - \frac{T_C(l)}{T_C(\infty)} \propto l^{-\lambda}. \tag{4}$$

Here $T_C(\infty)$ is the bulk critical temperature and λ has a value between 1.0 and 2.0 depending on the spin model used and the type of calculation. For thick films, λ is expected to be $1/\nu^{3d}$.[32] A better fit for films of a range of thicknesses l is given by Ref. 39 and has the form

TABLE I. Fitting parameters for Ising thin films using Eq. (5). MC and MF stand for Monte Carlo and mean field, respectively. Notice that $1/\nu^{3D}$ here are in good agreement with previous studies and exact results.

	Structure	$T_C(\infty)$	$\lambda(\infty) = 1/\nu^{3D}$
MC	sc	$4.539 \pm 6 \times 10^{-3}$	$1.578 \pm 3 \times 10^{-3}$
	bcc	$6.389 \pm 3 \times 10^{-3}$	$1.620 \pm 1 \times 10^{-2}$
	fcc	$9.860 \pm 2 \times 10^{-2}$	$1.621 \pm 8 \times 10^{-3}$
MF	sc	$6.0020 \pm 2 \times 10^{-4}$	$2.002 \pm 4 \times 10^{-3}$
	bcc	$8.0320 \pm 4 \times 10^{-3}$	$2.002 \pm 2 \times 10^{-3}$
	fcc	$12.0500 \pm 6 \times 10^{-3}$	$2.000 \pm 2 \times 10^{-3}$

$$\frac{1}{T_C(l)} = \frac{1}{T_C(\infty)}\left[1 + \left(\frac{l_0}{l - l'}\right)^{\lambda'}\right], \tag{5}$$

where l_0, l', and λ' are all adjustable parameters. Similarly, λ' should tend to $1/\nu^{3D}$ as $l \to \infty$. Using Eq. (5) we fit the $T_C(l)$'s arising from our Monte Carlo calculations. If it turns out that our $T_C(l)$'s are accurate and that the fit is a useful one, we should find $T_C(\infty)$ in agreement with the T_C^{bulk} we have calculated separately. Results of the fit are shown in Table I, and there is less than a 1% difference between $T_C(\infty)$ and T_C^{bulk} for all three types of films. However, even for $l = 20$, it turns out that λ' is not close to the expected large l value, $1/\nu^{3D}$. To elucidate further the evolution from 2D- to 3D-like behavior we rearrange the power law of Eq. (4) and define

$$\lambda_{\mathrm{eff}}(l_i) = -\log\left(\frac{T_C(\infty) - T_C(l_i)}{T_C(\infty) - T_C(l_{i-1})}\right) \Bigg/ \log\left(\frac{l_i}{l_{i-1}}\right), \tag{6}$$

and tabulate $\lambda_{\mathrm{eff}}(l_i)$ with l_i for our Monte Carlo simulations ($l_i \in \{4,6,8,10,15,20\}$) [and also for comparison the mean-field calculations (l_i ranging from 4 to 20 layers)]. The λ_{eff}'s should converge to the asymptotic shift exponents $1/\nu^{3D}$ when l tends to infinity. A linear least-squares fit between $\lambda_{\mathrm{eff}}(l_i)$ and $1/l_i$ enables us to obtain $\lambda_{\mathrm{eff}}(\infty)$ which is also given in Table I. The mean-field values of $\lambda_{\mathrm{eff}}(\infty)$ for all structures all have values of 2 since the mean field ν is well known to be 1/2. For the Monte Carlo simulation results, it is gratifying to find $\lambda_{\mathrm{eff}}(\infty)$ to be close to $1/\nu^{3D}$ which we obtain from separate bulk Monte Carlo simulations. This gives good support to the contention of universality and the asymptotic behavior contained in Eqs. (4) and (5).

C. Critical exponents

The effective critical exponents can be extracted from Eq. (3) as well as $dU_L/d\beta$, against L at T_C. This is actually the first test of the validity of the empirical formula, Eq. (3). Results from our simulations, at T_C, indeed show very good linear relationships between $\log_2 m$, $\log_2 \chi$, and $\log_2 dU_L/d\beta v$ with $\log_2 L$ for all our thin-film thicknesses and structures, e.g., in Fig. 2. We note here that $dU_L/d\beta \propto L^{1/\nu'}$. The exponents β'/ν', γ'/ν', and $1/\nu'$ can be extracted from the slopes of the linear least-squares fits. For the

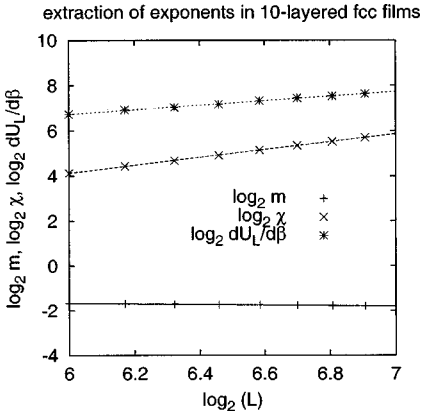

FIG. 2. An example of the extraction of effective critical exponents β', γ'/ν', and $1/\nu'$ from the slope of a least-square fit (see text) for ten-layered fcc films. The apparent linear relation supports Eq. (3).

second test, we perform the calculation of the effective dimension $d_{\text{eff}}=\gamma'/\nu'+2\beta'/\nu'$. We have found that, in each case, d_{eff} has a value of 2 within error bars as shown in Fig. 3 as expected. This confirms the 2D universality in thin films and ensures the possibility of using Eq. (3) to describe the critical behavior of the thin films. For the last test, we consider the scaling functions in Eq. (3). We calculate these scaling functions for the ten-layered sc films with $L=10$, 20, 40, 60, 80, 100, 150, and 200 using the exponents extracted from $L=64$ to 128. The results are shown in Fig. 4. For large enough L ($L=60-200$), excellent data collapses occur. This ensures that our effective critical exponents are reliable. *However, in the same figure for small L* (*around* $L=10$ *and* 20), *data collapsing is not found. This is what we must expect since the* 2D *universality is compromised when L approaches l.*

Since our results pass all of the three tests above, it is reasonable to propose Eq. (3) to be very useful for extracting effective critical exponents for film systems at T_C. Moreover, we find that the exponents γ'/ν' and β'/ν', for $l=1$ up to

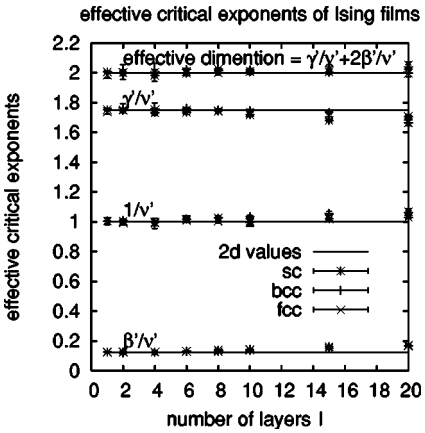

FIG. 3. Results of effective critical exponents for all sc, bcc, and fcc films. The exponents are close to 2D values. Especially, for thin films ($l\leqslant 8$), they are consistent with 2D results. That $d_{\text{eff}}=\gamma'/\nu'+2\beta'/\nu'\simeq 2$ also confirms 2D universality.

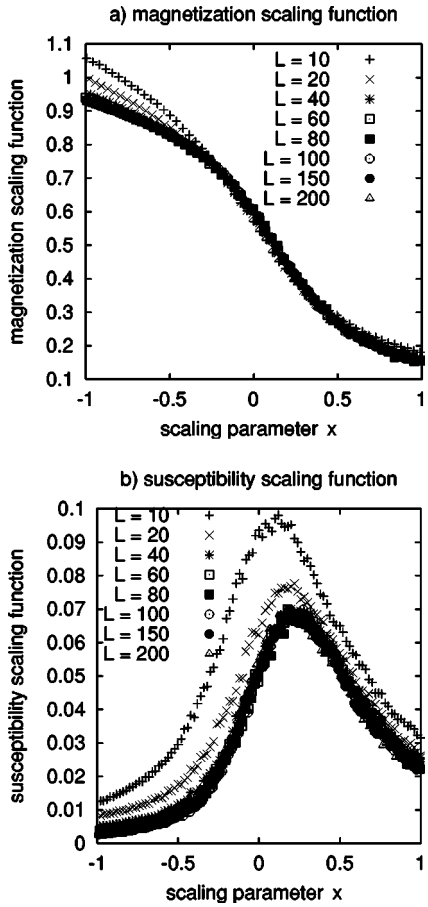

FIG. 4. The scaling functions for the magnetization (a) and susceptibility (b) in ten-layered sc systems with L from 100 to 200 calculated by using those effective exponents extracted for ten-layered sc films with L ranging from 64 to 128. A good collapse of the data is found for all systems with $L\geqslant 60$ including $L=150,200$ which are bigger than those used in the effective exponent extraction. Note, however, that for $L\rightarrow l=10$, the collapse becomes very poor because the 3D behavior (which is different from thin-film properties—i.e., 2D like) becomes more important at the limit $L\gg l$. Here, the reduced temperature $t=T/[T_C(l=10)]-1$.

$l=20$ films, are quite close to their 2D values as shown in Fig. 3. In particular, for thin films ($l\leqslant 8$), the exponent values seem to be almost identical to the 2D results. On the other hand, for thicker films ($l\geqslant 10$), a weak dependence of the exponents on l is found in agreement with, Refs. 16 and 17. This is somewhat reasonable since L is no longer much larger than l and corrections to scaling may be needed. In addition, we find that the thicker the film, the greater the difference from 2D. Inevitably, for studies of thick films which still produce 2D-like results, very large L's are required which are not computationally feasible. Nevertheless, from thin films with thicknesses of around eight layers and thinner, the effective exponents are very close to the 2D values. Thus, we feel safe in concluding that thin films belong to the 2D class. In addition, our results show that, at a good level of agreement, the effective critical exponents from all structures represent the same universality class.

Next, to elucidate further our conclusions about the critical exponents, we consider the relevant scaling functions (for

TABLE II. The effective critical exponents from the collapse of the scaling functions for sc films with thickness varying from monolayer to eight layers. At a particular thickness, *l is fixed and* $L \geqslant 10 \times l$ *are used to find the collapse*. The prime indicates the effective critical exponents for their corresponding parameters. The best collapsing (smallest P_b) is used to extract an optimum set of the effective exponents. Errors (Ref. 40) are in a unit of the last digit.

No. layers	χ		m	
	$1/\nu'$	γ'/ν'	$1/\nu'$	β/ν'
1	1.00	1.76	1.02	0.124
2	1.02	1.76	1.02	0.130
4	1.02	1.76	1.00	0.138
6	1.04	1.77	1.00	0.148
8	1.08	1.79	1.00	0.159

magnetization and susceptibility) and extract the effective critical exponents from data collapses. Figure 4 provides a useful visual preview, but we now measure the quality of a data collapse method according to Ref. 40 who defined

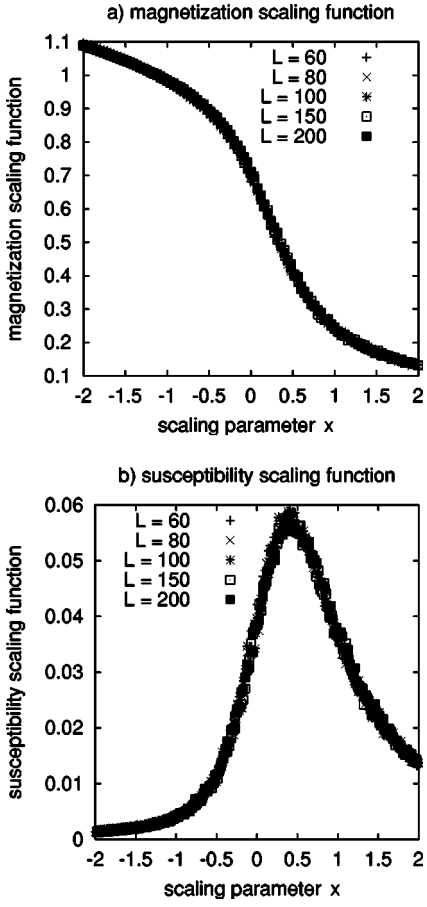

FIG. 5. The collapsing of magnetization and magnetic susceptibility scaling function *using Eq.* (7) *for fixed* $l=6$ *sc films with varying* $L=\{60,80,100,150,200\}$. The best collapsing gives $1/\nu'=1.04$, $\gamma'/\nu'=1.77$ for susceptibility and $1/\nu'=1.00$, $\beta'/\nu'=0.148$ for magnetization. Here, the reduced temperature $t=T/[T_C(l=6)]-1$.

TABLE III. The effective critical exponents extracted from the collapse of the scaling functions for sc films with the ratio l/L varying from 1.00 to 0.05. At a particular ratio l/L, l/L is *fixed* and the effective critical exponents from both varying L and l are presented. Errors (Ref. 40) are in a unit of the last digit. Notice that the results are close to 3D values.

Ratio l/L	Varying L				Varying l			
	χ		m		χ		m	
	$1/\nu'$	γ'/ν'	$1/\nu'$	β'/ν'	$1/\nu'$	γ'/ν'	$1/\nu'$	β'/ν'
1.00	1.54	1.94	1.69	0.502	1.54	1.94	1.64	0.521
0.50	1.53	1.93	1.64	0.509	1.60	1.94	1.63	0.522
0.33	1.49	1.92	1.63	0.508	1.59	1.92	1.63	0.509
0.25	1.51	1.95	1.61	0.509	1.60	1.93	1.61	0.515
0.20	1.75	2.00	1.61	0.509	1.59	1.92	1.61	0.515
0.10	1.64	2.00	1.60	0.484	1.57	1.92	1.60	0.491
0.05	1.78	1.98	1.58	0.463	1.57	1.91	1.58	0.465

$$P_b = \left[\frac{1}{N_{\text{over}}} \sum_p \sum_{i \neq p} \sum_{i_{\text{over}}} |L_j^{\beta'/\nu'} m_{i,j} - \varepsilon_p(L_j^{1/\nu'} t_{ij})| \right], \quad (7)$$

where m_{ij} is the ith value of the magnetization for the jth set of L (i.e., $L=L_j$ for set j) and t is the reduced temperature. $\varepsilon_p(x)$ is the interpolating function based on the values of set p and N_{over} is the number of pairs. Any extrapolation is avoided. From this, we are allowed to extract the exponents from where all scaling functions have the best collapse (i.e., at a right choice of β' and ν', P_b will be smallest) for both magnetization and susceptibility. For the susceptibility, we change m_{ij} to χ_{ij} and $L_j^{\beta'/\nu'}$ to $L_j^{-\gamma'/\nu'}$.

Clearly Eq. (7) is very useful for extracting the best exponents corresponding to the scaling data and the form of the scaling functions. For further analysis, we consider several forms of scaling functions, which allows us to track the critical information from different aspects, as follows:

(i) l is fixed and $L \geqslant l$ (e.g., we use $L \geqslant 10 \times l$) are used to find the scaling functions

$$m(T \to T_C(l), L, l) = L^{-\beta'/\nu'} \tilde{m}(tL^{1/\nu'}, l),$$

$$\chi(T \to T_C(l), L, l) = L^{\gamma'/\nu'} \tilde{\chi}(tL^{1/\nu'}, l); \quad (8)$$

e.g., see results in Table II and Fig. 5.

(ii) l/L is fixed and $L \geqslant 4$ are used to consider the scaling functions in the form

$$m\left(T \to T_C(l), L, \frac{l}{L}\right) = L^{-\beta'/\nu'} \tilde{m}\left(tL^{1/\nu'}, \frac{l}{L}\right),$$

$$\chi\left(T \to T_C(l), L, \frac{l}{L}\right) = L^{\gamma'/\nu'} \tilde{\chi}\left(tL^{1/\nu'}, \frac{l}{L}\right); \quad (9)$$

e.g., see results in Table III and Fig. 6.

(iii) l/L is fixed and use $l=\{1,2,4,6,8\}$ to consider the scaling functions in the form

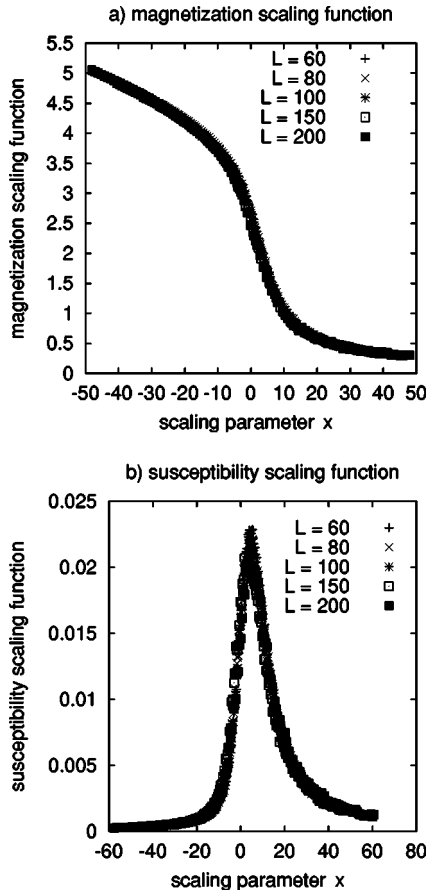

FIG. 6. The collapsing of magnetization (a) and magnetic susceptibility (b) scaling function *at the ratio* $l/L=0.1$ for sc films *with varying* $L=\{60,80,100,150,200\}$. Here, the reduced temperature $t=T/[T_C(l=0.1L)]-1$.

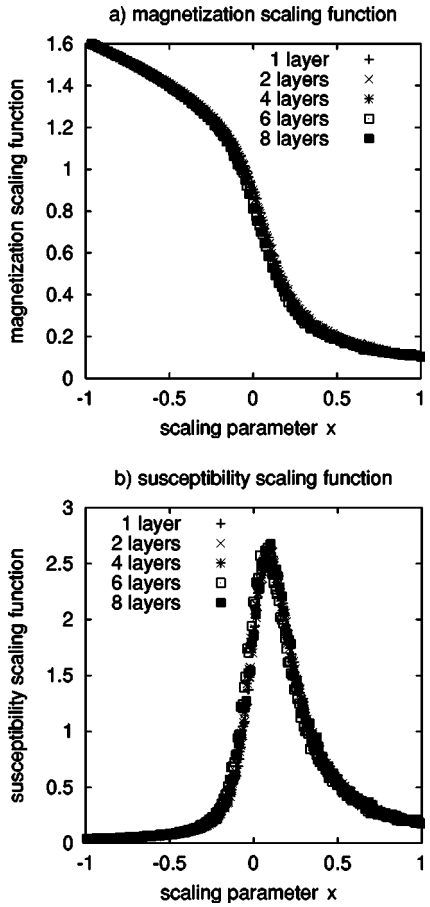

FIG. 7. The collapsing of magnetization (a) and magnetic susceptibility (b) scaling function *at the ratio* $l/L=0.1$ for sc films *with varying* $l=\{1,2,4,6,8\}$. Here, the reduced temperature $t=[T/T_C(l)]-1$.

$$m\left(T\to T_C(l),l,\frac{l}{L}\right)=l^{-\beta'/\nu'}\tilde{m}\left(tl^{1/\nu'},\frac{l}{L}\right),$$

$$\chi\left(T\to T_C(l),l,\frac{l}{L}\right)=l^{\gamma'/\nu'}\tilde{\chi}\left(tl^{1/\nu'},\frac{l}{L}\right), \qquad (10)$$

e.g., see results in Table III and Fig. 7.

(iv) From the magnetization and magnetic susceptibility scaling functions—i.e., $\tilde{m}(l)$ and $\tilde{\chi}(l)$—we try to make all scaling functions from $l=\{1,2,4,6,8\}$ collapse onto a same curve; that is, we write

$$\tilde{m}(l,x\to x_C)=l^{-j}\tilde{\tilde{m}}(x'), \quad \tilde{\chi}(l,x\to x_C)=l^{i}\tilde{\tilde{\chi}}(x'), \quad (11)$$

where $\tilde{\tilde{m}}$ and $\tilde{\tilde{\chi}}$ are the scaling functions of the usual scaling functions $\tilde{m}(l,x)$ and $\tilde{\chi}(l,x)$. Here $x=(T/T_C(l)-1)\times L^{1/\nu'}$ is the scaling parameter. Using a trial and error method, we found $x'=(x+x_c)\times l^k$. Here x_c, i, j, and k are all adjustable parameters used to find the best collapse. Results are shown in Fig. 8.

For this scaling function study, we performed extensive extra simulations for Ising sc films with L ranging from 4 to 200 and l from monolayer up to 20 layers. Up to 201 data from different temperatures in each system were collected to make the scaling. However, due to limitations in computational resources, only 5000 equilibrium configurations in each simulation were collected to make the average. In the calculation of P_b, at least 4 different scaling functions are required in order to consider the collapse. One may also notice that we have set $L\geqslant 10\times l$ in the first scaling form since we require $L\gg l$ and, because of computer limitations, we can extract the exponents up to only $l=8$ from $\tilde{m}(T,L\geqslant 10l,l)$ and $\tilde{\chi}(T,L\geqslant 10l,l)$.

Table II demonstrates that for fixed l, the effective critical exponents are close to those we extract from the empirical finite size scaling analysis. For fixed l/L but varied l or L (the second and the third scaling form), the correlation length ξ can now expand in the 3D-like manner. As can be seen in Table III, the extracted exponents are close to the 3D values as expected. For the collapsing of the scaling functions in Fig. 8 (the last scaling form), the exponents i, j, and k are not close to 2D values. This may indicate that corrections to scaling are needed. Nevertheless, the quality of our data does not allow us to perform trial fits with these extra parameters. However, we can see that it is possible to perform simulation for a number of finite systems only and then be able to describe critical behavior of other systems via some suitable scaling functions.

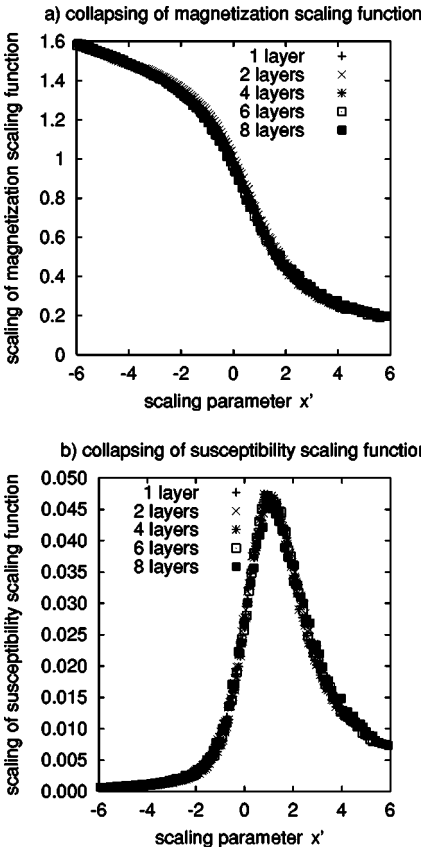

FIG. 8. The collapsing of *magnetization scaling function* (a) and *magnetic susceptibility scaling function* (b) scaling function (based on $L=200$) for sc films *with varying* $l=\{1,2,4,6,8\}$. With Eq. (11), for susceptibility, it is found that $x_c=0.11$, $k=0.46$, $i=-0.13$, and $P_b=0.002$. For magnetization, $x_c=-0.07$, $k=0.54$, $j=0.21$, and $P_b=0.03$. Here, the reduced temperature $t=[T/T_C(l)]-1$.

Finally, we compare our results for the effective exponent β' with those available from experiment on Ni films.[6] As shown in Fig. 9, the experimental results are close to ours—i.e., 2D like only for films thinner than four layers. If the Ni experiment can be described using the Heisenberg model, this behavior is not surprising because the anisotropic

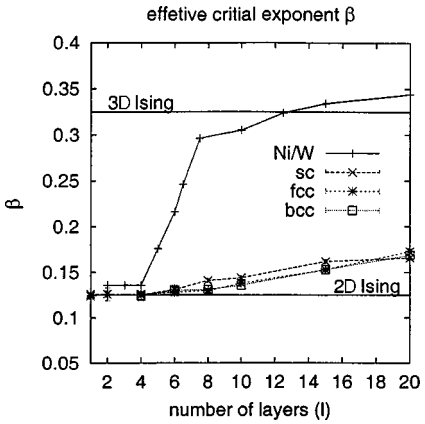

FIG. 9. Comparison of the effective critical exponent β extracted from experimental data for Ni(111)/W(110) in Ref. 6 and from Monte Carlo simulations of Ising thin films.

Heisenberg magnet becomes Ising like only for very thin films. However, a strange behavior of a sharp dimensional crossover of β at around five to eight layers is found,[6] whereas infinitely large films should belong to the 2D class for any thicknesses.

On the other hand, our results show a slight increase of β'/ν' towards its bulk value from $l=10$ onwards because L is still finite. Hence with increasing l the 3D character of the films becomes prominent and β' is dragged away from the 2D limit. This can be interpreted as an evidence of a crossover due to the shape effect. As a result, our finite-size simulations suggest the crossover from 2D to 3D Ising, but the dimensional crossover of β in Ref. 6 may be a transition from 2D Ising to 3D Heisenberg. So a direct comparison may not be allowed. That said, the sharp increase at five to eight layers in Ref. [6] that is not found from our results is quite an interesting issue. Although Ising and Heisenberg films may be quantitatively different, they should qualitatively share the same characteristics since, in the critical region, the divergence of the correlation length ξ in both models should be 2D like. So it is strange that β in Ref. 6 should change its value so abruptly with very few layers. To find more answers, we consider Ref. 13 (Schilbe *et al.*, 1996) which claimed "the author of Ref. 6 neglected the dependence of the (effective) critical exponents away from the critical point on the reduced temperature in their evaluation of the experimental data." In other words, the range of temperatures $10^{-3}<t<10^{-1}$ used for the power law fit in Ref. 6 may not belong to the asymptotic behavior (critical region), and the fit may lead to somewhat dubious results. So, to investigate this closely, we follow Ref. 13 who defined

$$\beta_{\text{eff}}=\frac{\partial \log m}{\partial \log t}, \tag{12}$$

and study how this quantity varies with t in thin films.

In the critical region of thin films—i.e., $l\ll\xi<L$—the finite-size effect upon 2D-like phenomena becomes important for $\xi\to L$. At a fixed l, the temperature range of this 2D-like phenomena depends on the value of ν', and $\xi\propto t^{-\nu'}$ will realize its finite limit at a temperature around $\log t=-(1/\nu')\log L$. To investigate this topic carefully, we calculate and plot β_{eff} against $\log_{10} t$ for $100\times100\times l$ films in Fig. 10. The rough pattern of the β_{eff} curves is in agreement with the investigations in Ref. 13. Since $L=100$ is used in our calculation, the β_{eff} are reliable (with minimum finite-size effect) only down to $\log_{10} t\simeq-2$. However, this range of $\log_{10} t$ does cover most of the range $-3<\log_{10} t<-1$ used in the power law fit in Ref. 6, and shows a quite interesting feature. It appears that this range of temperatures is not in the critical region because β_{eff} for each film is not constant, but peaks at a certain temperature. Outside the critical region (paramagnetic side), the correlation length grows as we increase the temperature towards T_C. As long as ξ is smaller than the film thickness, the film tries to behave as the 3D bulk system and β_{eff} grows somewhat towards the bulk value $\beta^{3D}\approx0.3258$.[26] However, at some temperature ξ becomes comparable with the film thickness and is only allowed to expand in the in-plane direction, exhibiting 2D-like behavior.

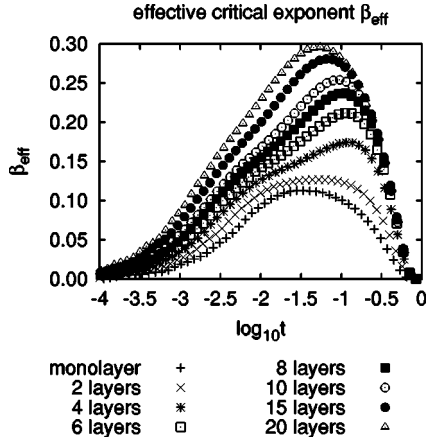

FIG. 10. The effective critical exponent β_{eff} extracted from $100\times100\times l$ sc Ising films where l is the number of layers. For $l \geqslant 4$, it is found that around $\log_{10} t=-1$ to -1.5, the β_{eff} curves reach peaks and this indicates how a steplike function of β of the form described in Ref. 6, i.e., Fig. 9, is possible. Here, the reduced temperature $t=1-T/T_C(l)$.

Thus, β_{eff} changes its trend and the resulting decrease results in a peak. We can also notice that the thicker the film, the closer the peak can grow towards the bulk value. It is certain if one tries to perform the power law fit for this temperature range, a sudden change of β_{eff} will be observed.

We may conclude that the range $-3<\log_{10} t<-1$ used for the power law fit in Ref. 6 is outside the critical region and thus the power law fit should not work well. This explains why the behavior of β in Ref. 6 does not really relate to our results because our studies concentrate on the critical region.

IV. CONCLUSION

We have studied the magnetic behavior of Ising thin films in sc, bcc, and fcc structures using extensive Monte Carlo simulations (and mean-field analysis). We have found the dimensional crossover of both m and χ from 2D to 3D like with increasing film thickness. The layer components of m and χ are found to have the lowest magnitudes at the surface while the innermost layers have the highest due to the free boundary effect at the surfaces. The film T_C's evolve from 2D to 3D values with increasing film thickness in good agreement with previous studies. The empirical fit of our calculated T_C's for films of varying l gives the fitted T_C at the limit of infinitely thick films which agrees very well with that calculated directly from separate 3D calculations. Another empirical fit for the shift exponent also suggests convergence to the 3D limit with increasing numbers of monolayers.

We have examined the critical regime of these systems in detail and extracted effective critical exponents via empirical formulas based on a finite-size scaling method for films. The validity of these formulas are successfully verified. The results show a very weak variation of the effective critical exponents with respect to l, the film thickness. For thin films ($l\leqslant 8$) the exponents are essentially the same as 2D and from this it can be implied that thin films fall into the 2D class. For thicker films, however ($l\geqslant 10$), a weak l dependence is noticeable because l is thick enough for the correlation length to distinguish the geometry of the films from that of a simple 2D lattice which is a consequence of a finite-shape effect.

We performed further analysis of our results using scaling functions of various forms and their data collapses. It is found that for fixed l but varying L, the effective critical exponents are close to those extracted from the empirical finite-size scaling analysis, but for fixed l/L, the exponents move to 3D values as expected. In addition, we consider the scaling functions for each thickness l and draw a general scaling form for the collapsing of those scaling functions.

Finally, in comparison with the experimental results described in Ref. 6 our results for the thinner films bear up well. A direct comparison, however, is not possible. This is because the experimental data from nickel films on a tungsten substrate can be interpreted to show a transition from 2D Ising to 3D Heisenberg rather than from 2D Ising to 3D Ising which is the only possibility for the model and systems we have studied here. There is also the issue that the experimental data used to make a power law fit are taken from temperatures that are outside the critical regime.

ACKNOWLEDGMENTS

We acknowledge the use of computer resources provided by the Center for Scientific Computing at the University of Warwick. One of us (Y.L.) would like to thank IPST (Thailand) for partial financial support.

[1] L. M. Falicov, D. T. Pierce, S. D. Bader, R. Gronsky, K. B. Hathaway, H. J. Hopster, D. N. Lambeth, S. S. P. Parkin, G. Prinz, M. Salamon, I. K. Schuller, and R. H. Victora, J. Mater. Res. **5**, 1299 (1990).

[2] M. T. Johnson, P. J. H. Bloemen, F. J. A. den Broeder, and J. J. de Vries, Rep. Prog. Phys. **59**, 1409 (1996).

[3] M. Bander and D. L. Mills, Phys. Rev. B **38**, 12 015 (1988).

[4] K. Binder and P. C. Hohenberg, Phys. Rev. B **9**, 2194 (1974).

[5] H. J. Elmers, J. Hauschild, H. Höche, U. Gradmann, H. Bethge, D. Heuer, and U. Köhler, Phys. Rev. Lett. **73**, 898 (1994).

[6] Y. Li and K. Baberschke, Phys. Rev. Lett. **68**, 1208 (1992).

[7] M. J. Dunlavy and D. Venus, Phys. Rev. B **69**, 094411 (2004).

[8] G. A. T. Allan, Phys. Rev. B **1**, 352 (1970).

[9] T. W. Capehart and M. E. Fisher, Phys. Rev. B **13**, 5021 (1976).

[10] D. O'Connor and C. R. Stephens, Phys. Rev. Lett. **72**, 506 (1994).

[11] D. L. Lin, H. Che, and Y. Xia, Phys. Rev. A **46**, 1805 (1992); D. L. Lin, H. Che, W. Lai, and T. F. George, Phys. Rev. E **49**, 2155 (1994); Y. Song, Y. Chen, J. Luo, and D. Xian, Phys. Lett. A **221**, 124 (1996); J. T. Ou, F. Wang, and D. L. Lin, Phys. Rev. E

56, 2805 (1997).
[12] K. Binder, Thin Solid Films **20**, 367 (1974).
[13] P. Schilbe, S. Siebentritt, and K. H. Rieder, Phys. Lett. A **216**, 20 (1996); P. Schilbe and K. H. Rieder, Europhys. Lett. **41**, 219 (1998); M. I. Marqués and J. A. Gonzalo, Eur. Phys. J. B **14**, 317 (2000); Nanotechnology **12**, 143 (2001).
[14] M. Krech and D. P. Landau, Phys. Rev. E **53**, 4414 (1996).
[15] K. Binder and J. S. Wang, J. Stat. Phys. **55**, 87 (1989).
[16] Y. Rouault, J. Baschnagel, and K. Binder, J. Stat. Phys. **80**, 1009 (1995).
[17] O. Dillmann, W. Janke, M. Müller, and K. Binder, J. Chem. Phys. **114**, 5853 (2001).
[18] U. Wolff, Phys. Rev. Lett. **62**, 361 (1989).
[19] H. Müller-Krumbhaar and K. Binder, J. Stat. Phys. **8**, 1 (1973).
[20] P. C. Hohenberg and B. I. Halperin, Rev. Mod. Phys. **49**, 435 (1977).
[21] P. L'Ecuyer, in *Handbook of Simulation: Principles, Methodology, Advances, Applications, and Practice*, edited by J. Banks (Wiley, New York, 1998).
[22] K. Entacher (unpublished).
[23] P. D. Coddington, Int. J. Mod. Phys. C **5**, 547 (1994).
[24] K. Binder, Z. Phys. B: Condens. Matter **43**, 119 (1981).
[25] A. M. Ferrenberg and R. H. Swendsen, Phys. Rev. Lett. **61**, 2635 (1988).
[26] A. M. Ferrenberg and D. P. Landau, Phys. Rev. B **44**, 5081 (1991).
[27] M. E .J. Newman and G. T. Barkema, *Monte Carlo Methods in Statistical Physics* (Clarendon Press, Oxford, 1999).
[28] V. Privman, in *Finite Size Scaling and Numerical Simulation of Statistical Systems*, edited by V. Privman (World Scientific, Singapore, 1990).
[29] K. Binder, in *Finite Size Scaling and Numbercal Simulation of Statistical Systems*, edited by V. Privman (World Scientific, Singapore, 1990).
[30] H. E. Stanley, *Introduction to Phase Transitions and Critical Phenomena* (Clarendon Press, Oxford, 1971).
[31] M. E. Fisher, in *Critical Phenomena*, Proceeding of the International School of Physics, "Enrico Fermi," Varenna, Italy, Course LI, edited by M. S. Green (Academic Press, New York, 1971).
[32] M. N. Barber, in *Phase Transitions and Critical Phenomena*, edited by C. Domb and J. L. Lebowitz (Academic Press, New York, 1983), Vol. 8.
[33] M. E. Fisher, Rev. Mod. Phys. **46**, 597 (1974).
[34] M. E. Fisher, Phys. Rev. **180**, 594 (1969).
[35] F. Freire, D. O'Connor, and C. R. Stephens, J. Stat. Phys. **74**, 219 (1994).
[36] Q. Hong, Phys. Rev. B **41**, 9621 (1990).
[37] J. Adler, J. Phys. A **16**, 3585 (1983) and references therein.
[38] W. Haubenreisser, W. Brodkorb, A. Corciovei, and G. Costache, Phys. Status Solidi B **53**, 9 (1972) and references therein.
[39] F. Huang, M. T. Kief, G. J. Mankey, and R. F. Willis, Phys. Rev. B **49**, 3962 (1994); S. Z. Wu, F. O. Schumann, G. J. Mankey, and R. F. Willis, J. Vac. Sci. Technol. B **14**, 3189 (1996).
[40] S. M. Bhattacharjee and F. Seno, J. Phys. A **34**, 6375 (2001).